N,*N*-Dimethylthioformamide and *N*,*N*-Dimethylthiocarbamoyl Chloride: Molecular Structure by Gas-Phase Electron Diffraction and ab Initio Molecular Orbital and Density Functional Theory Calculations

Tore H. Johansen* and Kolbjørn Hagen

Department of Chemistry, Norwegian University of Science and Technology, NTNU, N-7491 Trondheim, Norway

Received: November 12, 2002; In Final Form: March 17, 2003

The molecular structures and the dimethyl rotamer properties of *N*,*N*-dimethylthioformamide (TFA) and *N*,*N*-dimethylthiocarbamoyl chloride (TCC) have been investigated using gas-phase electron diffraction (GED) data recorded at a temperature of 25 °C, together with ab initio molecular orbital (MO) and density functional theory (DFT) calculations, as well as normal coordinate analysis (NCA) using MP2/6-31+G(d,p) scaled force fields. The molecules exist in the gas phase as a single near-planar conformer, not exhibiting true C_s symmetry. The orientation of the two methyl groups on the nitrogen atom have been closely examined by ab initio MO and DFT calculations, and these have been found to be oriented differently in the two molecules. Relevant structural parameter values obtained from the GED refinements, using values from the MP2/6-31+G(d,p) calculations as constraints, were as follows (values under C_1 symmetry assumption with estimated 2σ uncertainties): For TFA, bond lengths (r_g) were r(C═S) = 1.649(2) Å, r(C_2−N) = 1.346(3) Å, r(⟨$C_{5,9}$−N⟩) = 1.463(2) Å (av), r(⟨C−H⟩) = 1.125(4) Å (av), bond angles ($\angle_\alpha$) were ∠NC_2S = 127.0(3)°, ∠⟨$C_2NC_{5,9}$⟩ = 121.8(5)° (av), ∠⟨$NC_{5,9}H$⟩ = 110.4(7)°, and torsion angle ϕ_1(S_3−C_2−N_1−C_5) = 12.8° ± 2.7°. For TCC, bond lengths (r_g) were r(C═S) = 1.641(3) Å, r(C_2−N) = 1.348(4) Å, r(C_2−Cl) = 1.772(4) Å, r(⟨$C_{5,9}$−N⟩) = 1.472(3) Å (av), r(⟨C−H⟩) = 1.109(8) Å (av), bond angles ($\angle_\alpha$) were ∠NC_2S = 127.4(6)°, ∠⟨$C_2NC_{5,9}$⟩ = 122.0(6)° (av), ∠⟨NC_2Cl⟩ = 113.0(4)°, and torsion angle ϕ_1(S_3−C_2−N_1−C_5) = −5.5° ± 10.1°. The results are discussed and compared with the oxygen analogues and previous results for the TCC molecule, as well as with similar molecules in the literature.

I. Introduction

The resonance effects that occur in the amides and thioamides, molecules with the general formula R′−C(═X)−NR_2 (X = O or S; Scheme 1), have been the source of some discussion over the years. This was evident in the study of the first thioamide, thioformamide (H−C(═S)−NH_2), which was studied by R. Sugisaki and co-workers in 1974[1], and in the study of thioacetamide (CH_3−C(═S)−NH_2) by M. Hargittai and co-workers in 1981[2]. The resonance effect in question may be illustrated by the forms **A**−**D** depicted in Scheme 1, for both the amide (**A**, **B**) and the thioamide (**C**, **D**) class of compounds.

The relative contribution to the overall structure from each of the resonance forms **A, B** or **C, D** in Scheme 1 would not be expected to be identical in the amide and the thioamides because of the different properties of the oxygen and the sulfur atoms. These properties are mainly the electronegativity and the relative size of the atomic orbitals used in the resonance bonding (stabilization) between the carbon atom and the oxygen or sulfur substituent. The resulting difference in relative resonance contribution to the structure has been the source of the discussion mentioned earlier. The main question is in which of these classes of compounds is the relative contribution from resonance form **B** (or the corresponding form **D**) the highest? A larger contribution from resonance form **B** (or **D**) would make a C to N bond with a larger degree of double bond character, see Scheme 1. A larger degree of double bond character would make the C−N bond distance shorter, and as a consequence, the amide or thiamide rotational barrier about this central bond would increase. There exist experimental data on the free-energy rotational energy barrier (ΔG*) for several corresponding amides and thioamides. These have been reviewed by Jackman[3]. Also, some gas-phase values for ΔG* obtained by M. Feigel by using ^{1}H NMR line shape analysis at 298 K[4] have been published. Taking the corresponding compounds *N*,*N*-dimethylacetamide (CH_3−C(═O)−$N(CH_3)_2$) and *N*,*N*-dimethylthioacetamide (CH_3−C(═S)−$N(CH_3)_2$) as an example, the gas-phase value for the central C−N free-energy rotational barrier in the acetamide was 15.6(2) kcal mol^{-1} while the value in the corresponding thioacetamide was 18.0(4) kcal mol^{-1} (at T = 330 K).[4] Several similar examples for amide−thioamide pairs showing the same increase in ΔG*[3] confirms a higher rotational barrier in the thioamides relative to corresponding amides. According to the arguments above, resonance form **D** of Scheme 1 would therefore contribute more to the structure of the thioamide than resonance form **B** would to the structure of the amide. The explanation for this difference in relative resonance contribution between the amides and the thioamides may in part be that the C═S double bond in the thioamides is weakened by a poorer orbital overlap in this bond compared to the more size-adapted atoms and therefore stronger orbital overlap in the C═O double bond.

SCHEME 1: Amide and Thioamide Resonance Structures

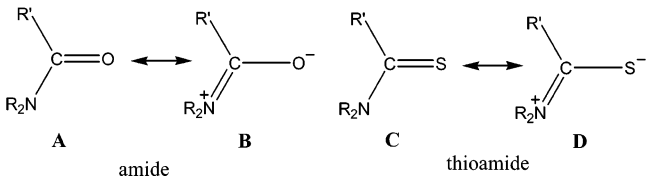

10.1021/jp022419c CCC: $25.00
Published on Web 05/15/2003

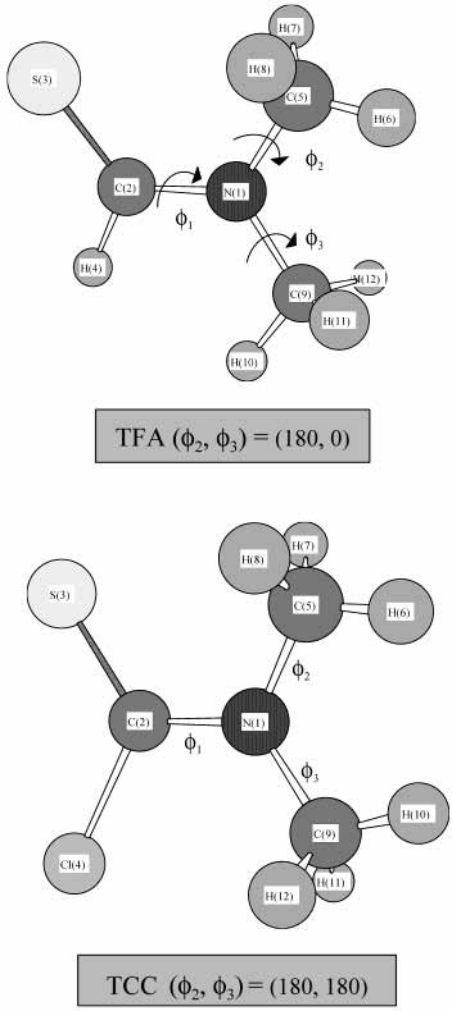

Figure 1. Molecular models of the minimum-energy rotamer of *N*,*N*-dimethylthioformamide (TFA; top figure) and of *N*,*N*-dimethylthiocarbamoyl chloride (TCC; bottom figure), including the atom numbering for each model.

The main geometrical parameters in these classes of molecules should reflect this difference in relative resonance form contribution. In most cases, this has been found to be true, as for instance in the longer r(C−N) bond distance value for acetamide (1.380(4) Å; r_g)[5] compared to the significantly shorter bond in thioacetamide (1.356(3) Å; r_g).[2] The nature of the substituent R′ in the general formula R′−C(═X)−NR_2 also has an influence on the rotational energy barrier and geometrical parameters. A highly electronegative R′ substituent (like −F, $-CF_3$, or −Cl) would most likely increase the rotational barrier and thus also decrease the central C−N bond distance, at least for the amide (X = O) class of compounds. An example of this is the gas electron diffraction (GED) work by I. Hargittai and G. Schultz on the molecule *N*,*N*-dimethylformamide (H−C(═O)−$N(CH_3)_2$)[6] and its halogenated counterpart, *N*,*N*-dimethylcarbamoyl chloride (Cl−C(═O)−$N(CH_3)_2$).[7] The value for r(C(O)−N) in the formamide was 1.391(6) Å (r_g),[6] while the corresponding value in the carbamoyl chloride, in which the H atom was replaced with the more electronegative Cl atom, was significantly lower at 1.365(3) Å (r_g).[7]

In this article, we present a continuation of the studies on these interesting compounds with the pair of molecules *N*,*N*-dimethylthioformamide (H−C(═S)−$N(CH_3)_2$, TFA; Figure 1) and *N*,*N*-dimethylthiocarbamoyl chloride (Cl−C(═S)−$N(CH_3)_2$, TCC; Figure 1). Results for the latter molecule were published by Naumov et al.[8] after our work was started, and a comparison

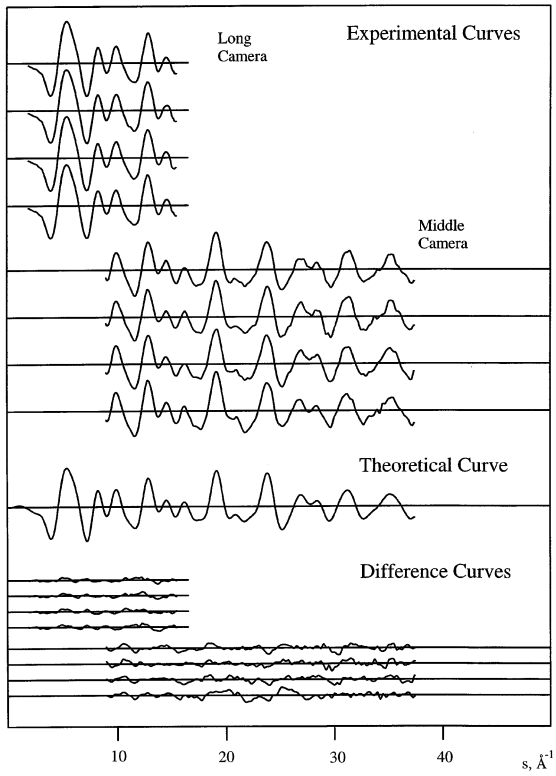

Figure 2. Intensity curves ($sI_m(s)$) for *N*,*N*-dimethylthioformamide (TFA). The experimental curves are the average molecular intensity data obtained from double tracings of each of the films from the two camera distances (long camera and middle camera). The theoretical curve was calculated from the structural parameters given in Table 2. The difference curves result from subtracting the relevant part of the theoretical curve from each of the experimental curves.

to their work will be made for TCC. Because we were interested in comparisons of results for TFA and TCC, we felt that the experimental conditions for the two experiments ought to be as similiar as possible. We therefore decided to continue the analysis of our data also for TCC. The present work was based on experimental GED data augmented with scaled quantum-mechanical (SQM) force fields at the ab initio MP2 level of theory, as well as extensive ab initio MO and density functional theory (DFT) calculations up to the level of MP4(SDQ) with a larger basis set to elucidate central and methyl rotational energy barriers and minimum-energy *N*,*N*-dimethyl orientations in the rotamers of the two title molecules.

II. Experimental Section

The samples of TFA and TCC were used as received from Fluka (98% (TFA), 99% (TCC)). Electron diffraction patterns for both compounds were recorded with the Oregon State University (OSU) gas-phase electron diffraction apparatus on Kodak Electron Image films with a nozzle-tip temperature of 298 K. Nominal accelerating voltage was 60 kV. Nozzle-to-film distances were 747.4 and 300.2 mm for the long camera (LC) and the middle camera (MC) distance experiments for TFA; the corresponding LC and MC distances were 747.1 and 299.9 mm for TCC. Sector-to-film distance was measured to 10.72 mm. The average electron wavelength was $\lambda = 0.048\,95$ Å for the TFA experiment and $\lambda = 0.048\,94$ Å for the TCC experiment. Four diffraction photographs from each of the LC and MC camera distances were used in the analysis of TFA, while three diffraction photographs from the LC and the MC camera distances were used in the analysis of TCC. A voltage/

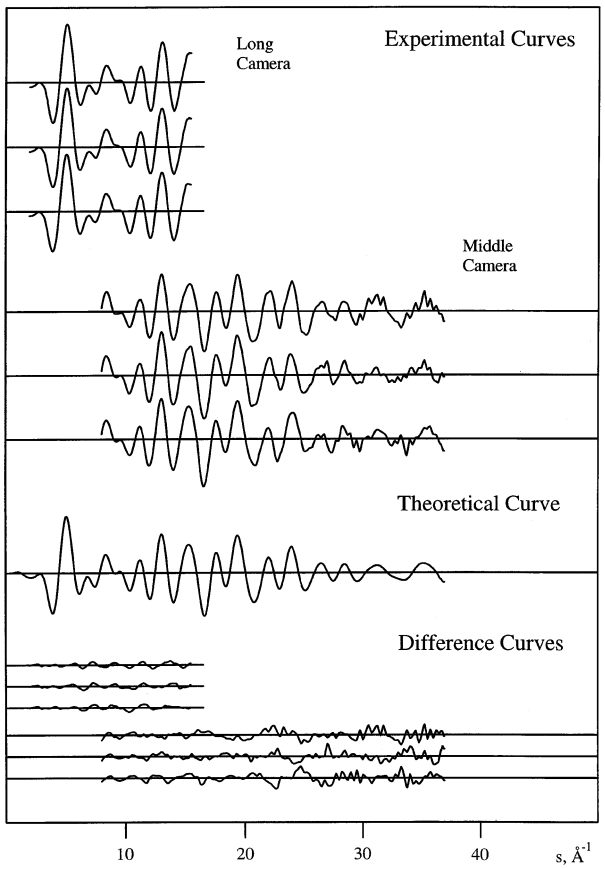

Figure 3. Intensity curves ($sI_m(s)$) for *N*,*N*-dimethylthiocarbamoyl chloride (TCC). The experimental curves are the average molecular intensity data obtained from double tracings of each of the films from the two camera distances (long camera and middle camera). The theoretical curve was calculated from the structural parameters given in Table 2. The difference curves result from subtracting the relevant part of the theoretical curve from each of the experimental curves.

distance calibration was made with CO_2 as reference (r_a(C═O) = 1.1646 Å; r_a(O···O) = 2.3244 Å). Each recorded film was scanned twice for optical densities, and the two scans were subsequently averaged. Optical densities were measured using the double-beam Joyce Loebl microdensitometer at OSU, and the data were reduced in the usual way.[9−11] The ranges of data finally used in the analyses were the following: For TFA, $2.00 \le s \le 15.50$ Å^{-1} and $9.00 \le s \le 37.50$ Å^{-1} for the LC and the MC distance experiments, respectively, and for TCC, $2.00 \le s \le 15.50$ Å^{-1} and $8.00 \le s \le 37.00$ Å^{-1} for the LC and the MC distance experiments, respectively. The data interval was $\Delta s = 0.25$ Å^{-1}.

For both molecules, a calculated background[12] was subtracted from the data for each film to yield experimental intensity curves in the form $sI_m(s)$. The individual data, one set from each of the films, are shown in Figure 2 for TFA and in Figure 3 for TCC, together with the final theoretical intensity curves and corresponding difference curves. In Figures 4 and 5 are shown the final experimental radial distribution (RD) curves for TFA and TCC, respectively, calculated in the usual way from the modified molecular intensity curves of the type $I'(s) = sI_m(s)Z_SZ_X(A_SA_X)^{-1}\exp(-0.0020\ s^2)$, where $A = s^2F$ and F is the absolute value of the complex electron scattering amplitudes (X = C for TFA; X = Cl for TCC). Theoretical intensity data were used for $s \le 1.75$ Å^{-1} in the experimental curves before the RD curves were calculated. The scattering amplitudes and phases were taken from tables.[13]

III. Structure Analysis

III.1. Ab Initio MO and DFT Calculations. Ab initio MO and DFT calculations were used to establish constraints in the GED models by incorporating some of the calculated geometrical differences as constants in the least-squares refinements. The geometries of TFA and TCC were fully optimized under a C_1 point group assumption, using Gaussian 98[14] and the following range of methods and basis sets: HF/6-311+G(d), HF/6-31+G(d,p), B3LYP/6-311+G(d), B3LYP/6-31+G(d,p), MP2(fc)/6-311+G(d), MP2(fc)/6-311++G(2d), MP2(fc)/6-31+G(d,p), and MP4(SDQ)/6-31+G(2d,p). In addition, we have calculated a series of four rotamer optimizations under a C_s symmetry constraint, as defined by the torsion angles

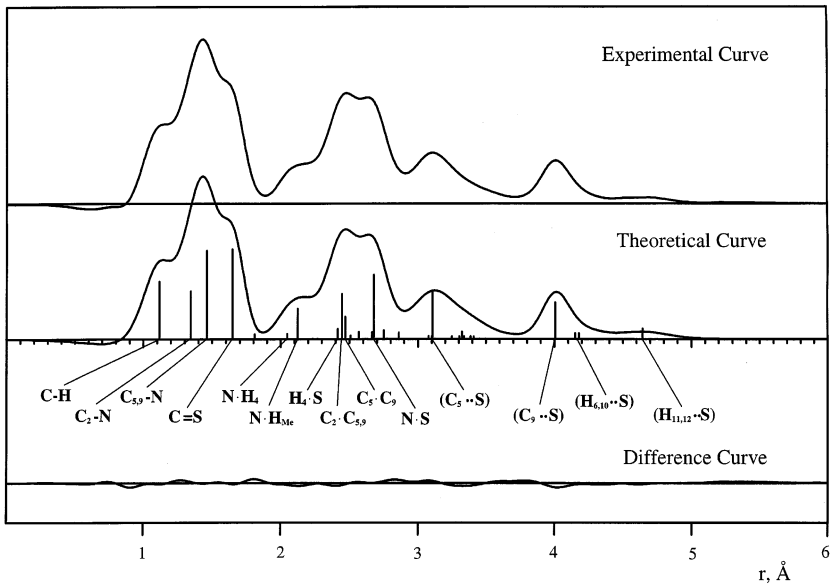

Figure 4. Radial distribution (RD) curves for *N*,*N*-dimethylthioformamide (TFA). The experimental curve was calculated from the composite of the two sets of average experimental curves (4LC + 4MC) shown in Figure 2 with the use of theoretical data for the region $0 \le s \le 1.75$ Å^{-1} and $B = 0.0020$ Å^2. The difference curve is the experimental curve minus the theoretical curve. The vertical lines indicate the distribution of interatomic distances; they have lengths proportional to the distance weights.

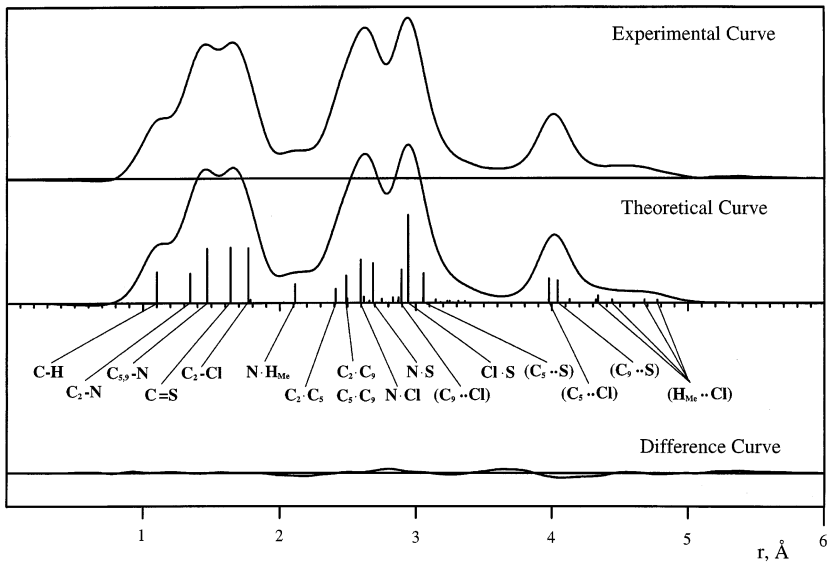

Figure 5. Radial distribution (RD) curves for *N*,*N*-dimethylthiocarbamoyl chloride (TCC). The experimental curve was calculated from the composite of the two sets of average experimental curves (3LC + 3MC) shown in Figure 3 with the use of theoretical data for the region $0 \le s \le 1.75$ Å^{-1} and $B = 0.0020$ Å^2. The difference curve is the experimental curve minus the theoretical curve. The vertical lines indicate the distribution of interatomic distances; they have lengths proportional to the distance weights.

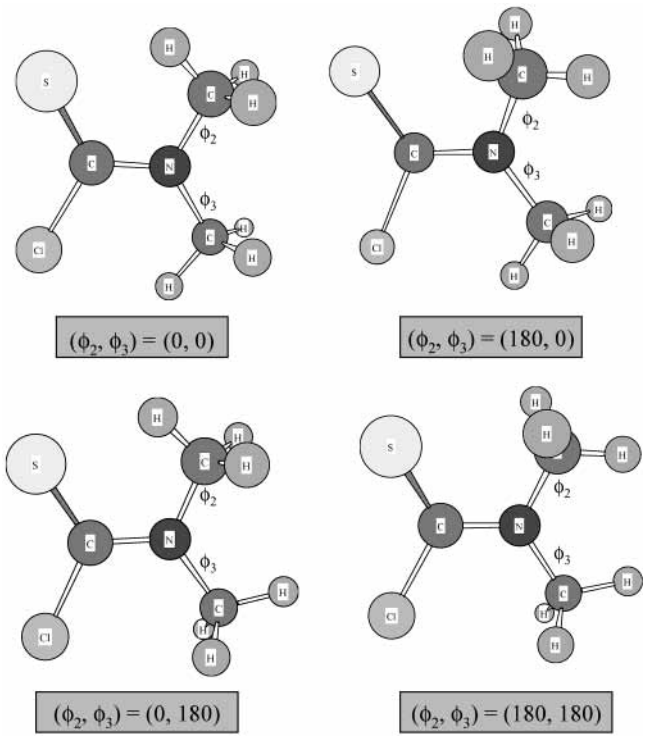

Figure 6. A series of four rotamers valid for both TFA and TCC, showing the label system $(\phi_2, \phi_3) = (a, b)$ used in this work.

(ϕ_2, ϕ_3) for the N−C_{Me} rotation as indicated in Figures 1 and 6, obtaining the number of imaginary normal modes given by the HF and MP2 level of theories using the basis set 6-31+G(d,p). The two methods differed on several occasions regarding the minima, HF giving true minima for some C_s rotamers while none of the C_s rotamers were characterized as true minima by the correlated MP2 method. Under a C_1 symmetry assumption, for which the torsional angles (ϕ_2, ϕ_3) for N−C_{Me} rotation may differ from the ideal values of 0° or 180° (or 60°), we have for simplicity retained the label system shown in Figures 1 and 6 for identifying the different *N*,*N*-dimethyl rotamers of the two molecules $((\phi_2, \phi_3) = (a, b)$; the complete definitions of the torsion angles are given in the next section). The resulting minimum-energy rotamers found by the series of C_1 calculations outlined above, given in the (ϕ_2, ϕ_3) label system, have been assembled in Table 1. The results were seen to differ systematically according to the method or basis set used or both, particularly for TCC. For all of these C_1 optimizations, frequency calculations were performed to ensure that a true rotamer minimum was obtained in each case, according to that particular calculation.

TABLE 1: Overview of All Unconstrained ab Initio MO and DFT Calculations Regarding the *N*,*N*-Dimethyl Group Orientations in *N*,*N*-Dimethylthioformamide (TFA) and *N*,*N*-Dimethylthiocarbamoyl Chloride (TCC), Showing the Obtained Minimum-Energy Rotamer under Full C_1 Symmetry in Each Case (in Label-type Form, See Figure 6)

calculation (C_1)	TFA rotamer (ϕ_2, ϕ_3)	TCC rotamer (ϕ_2, ϕ_3)
	HF	
6-311+G(d)	(180, 0)	(180, 0)
6-31+G(d,p)	(180, 0)	(180, 0)
	DFT/B3LYP	
6-311+G(d)	(180, 0)	(180, 0)
6-31+G(d,p)	(0, 0)	(180, 180)
	MP2(fc)	
6-311+G(d)	(180, 0)	(180, 0)
6-311++G(2d)	(180, 0)	(180, 180)
6-31+G(d,p)[a]	(180, 0)	(180, 180)
	MP4(SDQ-fc)	
6-31+G(2d,p)	(180, 0)	(180, 180)

[a] These were the unconstrained (C_1) MP2 calculations used as a parameter and force field basis in the GED analyses. All of these calculations showed no imaginary normal modes of vibration.

The potential energy curves for rotation about the central C(S)−N bond in TFA and TCC were also calculated using fixed steps of 15° from $\phi_1 = \phi$(C(S)−N) = 0 to 90° at the MP2/6-31+G(d,p) level of theory. These results are shown in Figure 7. Some geometrical results from the MP2/6-31+G(d,p) calculations were used in the actual GED least-squares refinements as constraints, together with the fixed-scaled MP2 force fields for both TFA and TCC (scale factor of 0.9 for all modes except out-of-plane and torsional vibrations; see next section). The MP2 calculations also gave zero-point vibrational energies (ZPE) for both compounds. These MP2 calculations, as well as the experimental results, are shown in Table 2. The geometrical

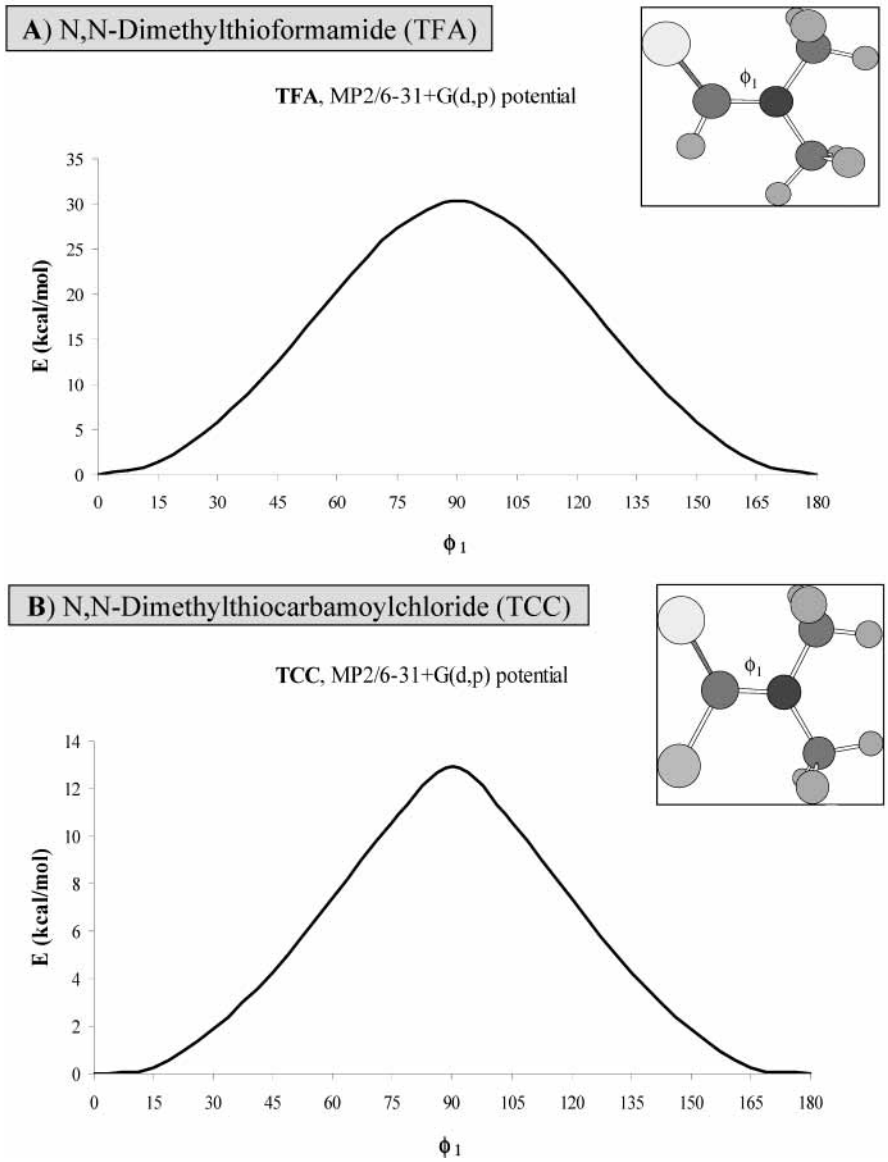

Figure 7. The calculated potential energy curves for rotation about the central C(S)−N bond in TFA (A) and TCC (B) (C_1 molecular symmetry) plotted using fixed steps of 15° from $\phi_1 = \phi(S_3-C_2-N_1-C_5) = 0-180$ ° at the MP2/6-31+G(d,p) level of theory. The actual 15° step values were calculated from 0° to 90° and then mirrored.

parameters and absolute energy results (corrected with the scaled ZPE values) of selected ab initio MO and DFT calculations (B3LYP, MP4(SDQ)) are shown in Table 3. The procedure of using ab initio MO results as constraints in GED analyses is well established.[15−17]

III.2. Gas Electron Diffraction Refinements. *Normal Coordinate Analysis (NCA).* The ab initio MO force fields calculated at the MP2/6-31+G(d,p) level were transformed from the original Cartesian coordinates to nonredundant internal (symmetry) coordinates and then scaled according to the types of internal coordinates using the scheme F_{ij}(scaled) = F_{ij}(ab initio) × $(X_iX_j)^{1/2}$, where X_i and X_j were the scale constants for the diagonal force constants. The single scale constant used was 0.9 for all modes of both TFA and TCC, except the three torsional vibrational modes and the two out-of-plane bending modes in each molecule because these modes were left unscaled. The MP2 SQM force fields were subsequently used in calculating shrinkage correction values and root-mean-square (rms) amplitudes of vibration (l) employed in the GED analyses. These calculations were performed using the later version of ASYM40.[18,19]

Refinements and Shrinkage Corrections. From the experimental RD curve and results from theoretical calculations, trial values for bond distances and bond angles were obtained for TFA and TCC. Refinements of the molecular structures based on the GED data were made by the least-squares method,[20] adjusting a theoretical $sI_m(s)$ curve calculated for each molecule simultaneously to the eight (TFA) and six (TCC) experimental intensity curves, one from each of the photographic films, using a unit weight matrix. The structures were converted from the geometrically consistent r_α to the r_a-type required by the formula for the theoretical scattered intensities ($r_a = r_g - l^2/r = r_\alpha - l^2/r + K_T + \delta r$),[21,22] by using values of the centrifugal distortion constants (δr), perpendicular amplitude corrections (K_T), and rms amplitudes of vibration (l) calculated at the temperature of the experiment, 298 K (25 °C).

The GED Molecular Parameters. The geometry of each of the thioamides can be described by a similar set of independent parameters, which were fitted to the experimental data. In our refinements, the independent parameters were chosen as ("⟨ ⟩" denotes average value) r(C═S), r(C_2−N), r(⟨C_{Me}−N⟩), r(⟨C−H⟩), r(C_2−Cl) (TCC only), ∠(NC_2S), ∠(⟨C_2NC_{Me}⟩), ∠(NC_2H_4)

TABLE 2: Experimental Results for TFA and TCC ($Me_2N-C(=S)X$; X = H, Cl) Obtained from the Least-Squares Refinements of the GED Data, along with Calculated Results at ab Initio MO MP2/6-31+G(d,p) Level of Theory[a]

	N,*N*-dimethylthioformamide (X = H)				*N*,*N*-dimethylthiocarbamoyl chloride (X = Cl)			
	gas electron diffraction/MP2		MP2/6-31+G(d,p) (unless otherwise noted)		gas electron diffraction/MP2		MP2/6-31+G(d,p) (unless otherwise noted)	
	r_g, $\angle_\alpha$	l_{exp}	r_e, $\angle_e$	l_{theo}	r_g, $\angle_\alpha$	l_{exp}	r_e, $\angle_e$	l_{theo}
$r(C{=}S)$	1.649 (2)	0.053 (3)	1.645	0.043	1.641 (3)	0.049 (5)	1.638	0.044
$r(C_2-N)$	1.346 (2)	0.046 (3)	1.350	0.044	1.348 (4)	0.047 (4)	1.355	0.045
$r(\langle C_{5,9}-N\rangle)$	1.463 (2)		1.455		1.472 (3)		1.464	
$r(\langle C_{5,9}-H\rangle)$	1.125 (4)		1.090		1.109 (8)		1.088	
$r(C_2-X)$	1.127 (4)	0.090 (5)	1.089	0.078	1.772 (4)	0.062 (6)	1.769	0.054
$\angle NC_2S$	127.0 (3)		127.0		127.4 (6)		126.4	
$\angle\langle C_2NC_{5,9}\rangle$	121.9 (5)		120.8		122.0 (6)		120.3	
ΔC_2NC_5[b]	[−0.3328]		−0.3328		[−3.2761]		−3.2761	
ΔC_2NC_9[b]	[+0.3328]		+0.3328		[+3.2761]		+3.2761	
$\angle NC_2X$	[112.3]		112.3		113.0 (4)		113.1	
$\angle\langle NC_{5,9}H\rangle$	110.4 (7)		109.7		109.6 (15)		109.7	
				Torsion				
$\phi_1(C_2-N)$[c]	12.8 (27)		3.1		−5.5 (101)		−4.5	
$\phi_2(N-C_5)$[d]	[−163.5]		−163.5		[173.2]		173.2	
$\phi_3(N-C_9)$[e]	[12.7]		12.7		[−171.4]		−171.4	
				Dependent				
$r(C_5-N)$	1.460 (2)	0.051 (3)	1.454	0.049	1.468 (3)	0.051 (4)	1.463	0.049
$r(C_9-N)$	1.465 (2)	0.051 (3)	1.456	0.049	1.476 (3)	0.051 (4)	1.465	0.050
$r(\langle C_5-H\rangle)$	1.123 (4)	0.089 (5)	1.089	0.078	1.108 (8)	0.086 (7)	1.088	0.077
$r(\langle C_9-H\rangle)$	1.125 (4)	0.090 (5)	1.090	0.078	1.110 (8)	0.086 (7)	1.087	0.077
$\angle C_2NC_5$	121.6 (5)		120.5		118.7 (6)		117.0	
$\angle C_2NC_9$	122.2 (5)		121.1		125.3 (6)		123.6	
$\angle\langle NC_5H\rangle$	110.1 (7)		109.5		109.4 (15)		109.5	
$\angle\langle NC_9H\rangle$	110.6 (7)		109.9		109.7 (15)		109.8	
$\angle C_5NC_9$	116.2 (9)		117.3		116.0 (12)		117.9	
$\angle S_3C_2X$	120.7 (3)		120.7		119.6 (4)		120.6	
$\angle HC_5H$	108.8 (7)		109.4		109.5 (15)		109.4	
$\angle HC_9H$	108.3 (7)		109.0		109.2 (15)		109.1	
$\sum CNC$	[360.0]		358.9 (MP2) 359.7 (MP4)[f]		[360.0]		358.5 (MP2) 360.0 (MP4)[f]	
				Methyl Energy Barriers				
$\Delta E(N-C_5)$[g]			0.17				0.53	
$\Delta E(N-C_9)$[g]			1.56				0.07	
R[h]	0.149				0.185			
R[i](theo)			0.267				0.210	

[a] Distances(r_g) and root-mean-square amplitudes of vibration (l) are in Å, and angles ($\angle_\alpha$) are in deg. Values in parentheses are 2σ, where σ include estimates of uncertainty in voltage/nozzle heights and of correlation in the experimental data. Values in brackets are taken from the respective ab initio MO calculations. [b] $\Delta C_2NC_5 = (\angle C_2NC_5 - \angle\langle C_2NC_{5,9}\rangle)$; $\Delta C_2NC_9 = (\angle C_2NC_9 - \angle\langle C_2NC_{5,9}\rangle)$. [c] $\phi_1 = \phi(S_3-C_2-N_1-C_5)$. [d] $\phi_2 = \phi(C_2-N_1-C_5-H_6)$. [e] $\phi_3 = \phi(C_2-N_1-C_9-H_{10})$. [f] MP4(SDQ)/6-31+G(2d,p) calculations, showing that the MP4(SDQ) level of theory gave practically totally planar structures. [g] Calculated methyl energy barriers to internal rotation (kcal mol^{-1}), including scaled zero-point energy differences between the ground and transition states (MP2 values; 1 kcal = 4.184 kJ (exact)). [h] The "goodness of fit" factor $R = [\sum w_i\Delta_i^2/\sum w_i(s_i I_m^{exp}(s))^2]^{1/2}$ and $\Delta_i = s_i I_m^{exp}(s) - s_i I_m^{calc}(s)$. [i] Obtained value for the R factor with the purely theoretical model (the MP2-based starting point for the GED refinement, including scaled shrinkage corrections).

(TFA only), $\angle(NC_2Cl)$ (TCC only), $\angle(\langle NC_{Me}H\rangle)$, $P(\angle HC_{Me}H)$ (projection angle in the methyl groups; the angle between two $C_{Me}-H$ bonds projected on a plane perpendicular to the $C_{Me}-N$ bond), and finally the torsional angle parameters $\phi_1 = \phi(S-C_2-N-C_5)$, $\phi_2 = \phi(C_2-N_1-C_5-H_6)$, $\phi_3 = \phi(C_2-N_1-C_9-H_{10})$, along with several difference parameters held at constant values obtained from the ab initio MO calculations using the MP2/6-31+G(d,p) results. The nonplanarity about the N atom was assumed to be zero (i.e., $\sum CNC = 360°$), as was indicated by the higher MP4(SDQ)/6-31+G(2d,p) calculations, see Table 2. The vibrational properties of the molecules were specified by 66 amplitude parameters, corresponding to the number of interatomic distances in each molecule. Some, but not all, of the amplitudes could successfully be refined. The amplitudes were refined together in groups depending on the interatomic distances. The amplitudes that could not be refined were kept constant at the values calculated from the MP2-based NCA calculations previously described. In the final refinements for TFA, seven geometrical parameters, one torsion parameter (ϕ_1), and six amplitude parameters were refined simultaneously. For TCC, nine geometrical parameters, one torsion parameter (ϕ_1), and eight amplitude parameters were refined simultaneously.

Results. The results of these refinements for both compounds are given in Table 2, along with the MP2/6-31+G(d,p) results. The minimum-energy rotamers are shown in Table 1. In Table 3, some of the more important MP4(SDQ) and B3LYP results have been assembled, and in Tables 4 and 5 selected experimental bonding and nonbonding interatomic distances are shown, together with corresponding MP2- and MP4(SDQ) distances. The correlation matrixes for the refined parameters are shown in Tables 6 and 7 for TFA and TCC, respectively. Experimental molecular parameters from several GED analyses for selected *N*,*N*-dimethylformamides and -thioformamides are assembled in Table 8. The theoretical intensity curve for the

TABLE 3: Calculated Molecular Parameters and Correlated Absolute Energies for *N*,*N*-Dimethylthioformamide (TFA) and *N*,*N*-Dimethylthiocarbamoyl Chloride (TCC) from DFT/B3LYP and MP4(SDQ) Computations[a]

	TFA (X = H)		TCC (X = Cl)	
parameter	B3LYP/6-31+G(d,p)	MP4(SDQ)/6-31+G(2d,p)	B3LYP/6-31+G(d,p)	MP4(SDQ)/6-31+G(2d,p)
r(C═S)	1.6602	1.6581	1.6482	1.6490
r(C$_2$−N)	1.3466	1.3393	1.3465	1.3407
r(C$_5$−N)	1.4576	1.4581	1.4702	1.4675
r(C$_9$−N)	1.4579	1.4573	1.4710	1.4689
r(C$_2$−X)	1.0927	1.0894	1.7979	1.7832
∠NC$_2$S	128.7	127.1	127.0	126.9
∠C$_2$NC$_5$	122.8	120.7	117.5	117.4
∠C$_2$NC$_9$	121.4	121.6	123.8	123.6
∠NC$_2$X	111.8	112.6	112.9	113.1
∠C$_5$NC$_9$	115.9	117.4	118.7	119.0
∠SC$_2$X	119.4	120.3	120.1	120.0
∠⟨NC$_{5,9}$H⟩	109.9	109.9	110.0	109.9
		Torsion		
ϕ_1(C$_2$−N)[b]	0.002	1.319	0.001	0.010
ϕ_2(N−C$_5$)[b]	0.036[d]	−166.4	180.0	180.0
ϕ_3(N−C$_9$)[b]	0.007[d]	6.301	180.0	180.0
E	−571.486 120	−570.470 288	−1031.075 953	−1029.516 805
ZPE[c]	0.100 123		0.090 819	
E + ZPE	−571.385 997		−1030.985 134	

[a] For atom numbering, see Figure 1. Distances (r) are in Å, and angles (∠, ϕ) are in deg; absolute energies (E) are in hartree/particle. [b] Torsion angles were defined as in the GED refinements (see Table 2). [c] Unscaled zero-point energy corrections from respective frequency analysis on the optimized geometries. All normal modes of vibration were found to be real. [d] This was the only calculation giving the rotamer (ϕ_2, ϕ_3) = (0, 0) for the dimethyl group orientation of TFA. All other calculations (DFT, HF, MP*n*) exclusively gave the (180, 0) orientation for TFA; see Table 1.

final model is shown in Figure 2 for TFA, together with experimental and difference curves for each film recorded. The corresponding intensity curves are shown in Figure 3 for TCC. The experimental and final theoretical RD curves along with the difference curves are shown in Figures 4 and 5 for TFA and TCC, respectively.

IV. Discussion

We have studied theoretically the rotational energy barrier heights for the methyl rotation about each of the N−C$_{Me}$ bonds and for the central rotation about the C(S)−N bond in TFA and TCC. The potential curves calculated at MP2/6-31+G(d,p) level of theory revealed quite different C(S)−N rotational barrier heights for the two molecules, see Figure 7. For TFA, the maximum energy value, $E(\phi_1$=90), was calculated to be 30.3 kcal mol^{-1} above the minimum energy value, $E(\phi_1$=0). The corresponding value calcuated for TCC was lower, at 12.9 kcal mol^{-1} for $E(\phi_1$=90). Experimental values for this rotational barrier exist for the amide analogues, *N*,*N*-dimethylformamide (H−C(O)−NMe$_2$)[23] and *N*,*N*-dimethylcarbamoyl chloride (Cl−C(O)−NMe$_2$),[4] in addition to the fluoro-substituted compound *N*,*N*-dimethylcarbamoyl fluoride (F−C(O)−NMe$_2$).[4] In contrast to our purely MP2 electronic energies, the experimental values were reported as the thermodynamic quantities ΔG^* or ΔH^* (free energy of activation and entalphy of activation, respectively). The ΔG^* values for *N*,*N*-dimethylformamide, *N*,*N*-dimethylcarbamoyl chloride and *N*,*N*-dimethylcarbamoyl fluoride were 19.4(1), 15.4(1), and 17.1(2) kcal mol^{-1}, respectively, in the gas phase at T = 298 K. Thus, ignoring the slight differences in defined quantities and experimental conditions, there was a reduction of approximately 11 kcal mol^{-1} in the central rotational barrier from the value calculated in TFA to the experimental value reported for its amide analogue but a slight increase in the rotational barrier of about 2.5 kcal mol^{-1} from the chlorinated thioamide TCC to its amide analogue. The fluoro-substitution increased this value further by about 1.7 kcal mol^{-1}, which was in accordance with the resonance arguments discussed previously for the presence of a higher electronegative substituent on the carbonyl carbon atom, see Scheme 1. However, in strong contrast to the experimental value of 15.4(1) kcal mol^{-1} found for the rotational energy barrier in *N*,*N*-dimethylcarbamoyl chloride, the semiempirical PM3 value reported by Naumov et al.[8] was less than 4 kcal mol^{-1}. The corresponding PM3 value calculated for TCC was in better agreement with our calculated MP2 value at about 14 kcal mol^{-1}.[8] In their work on *N*,*N*-dimethylformamide and *N*,*N*-dimethylacetamide,[23] Wiberg et al. calculated the methyl rotational barriers at the HF/6-31+G(d,p) level. They found values of 0.8 and 1.9 kcal mol^{-1} for the ground-state barriers of N−Me(syn) and N−Me(anti), respectively, where syn and anti refers to the position of the N−Me bond in relation to the C═O bond. Thus, a lower barrier height was found when the N−Me bond was syn to the C═O bond in the formamide. This was in accordance with our MP2 calculated results for TFA, see Table 2. We calculated the corresponding barrier values for TFA as 0.17 and 1.56 kcal mol^{-1} for N−Me(syn) and N−Me-

TABLE 4: Selected Bonding and Nonbonding Interatomic Distances and Vibrational Amplitudes from GED Refinements, along with Corresponding MP2 and MP4(SDQ) Distances for *N*,*N*-Dimethylthioformamide (TFA; Symmetry C_1)[a]

	GED				theoretical calculations	
	r_α	r_g	l_{exp}	l_{calc}[e]	r_e[f]	r_e[g]
			Bonding			
r(C═S)	1.643(2)	1.649	0.053(3)	0.043	1.645	1.658
r(C$_2$−N)	1.342(2)	1.346	0.046(3)[b]	0.044	1.350	1.339
r(C$_5$−N)	1.454(2)	1.460	0.051(3)[b]	0.049	1.454	1.458
r(C$_9$−N)	1.455(2)	1.465	0.051(3)[b]	0.049	1.456	1.457
r(C$_2$−H)	1.109(4)	1.127	0.090(5)	0.078	1.089	1.089
			Torsion Independent			
N$_1$·S$_3$	2.675(4)	2.680	0.064(3)	0.058	2.684	2.688
N$_1$·H$_4$	2.039(4)	2.052		0.098	2.031	2.025
C$_2$·C$_5$	2.440(6)	2.443	0.074(4)[c]	0.065	2.435	2.432
C$_2$·C$_9$	2.449(6)	2.454	0.072(4)[c]	0.064	2.444	2.442
C$_5$·C$_9$	2.470(13)	2.473	0.082(4)[c]	0.074	2.485	2.491
S$_3$·H$_4$	2.406(5)	2.415		0.100	2.392	2.400
			Torsion Dependent			
			Two Angles			
C$_5$··S$_3$	3.106(10)	3.109	0.117(6)[d]	0.116	3.080	3.086
C$_5$··H$_4$	3.381(7)	3.389		0.098	3.371	3.371
C$_9$··S$_3$	4.005(6)	4.006	0.067(4)[d]	0.066	4.010	4.023
C$_9$··H$_4$	2.558(11)	2.571		0.135	2.534	2.535
C$_2$··H$_6$	3.334(9)	3.341		0.105	3.300	3.302
C$_2$··H$_7$	2.666(15)	2.671		0.178	2.627	2.653
C$_2$··H$_8$	2.876(13)	2.884		0.228	2.866	2.845
C$_2$··H$_{10}$	2.574(17)	2.582		0.139	2.527	2.529
C$_2$··H$_{11}$	3.102(11)	3.113		0.184	3.086	3.123
C$_2$··H$_{12}$	3.244(10)	3.254		0.138	3.219	3.189
			Three Angles			
S$_3$···H$_6$	4.150(9)	4.155		0.122	4.120	4.140
S$_3$···H$_7$	2.768(19)	2.775		0.261	2.764	2.820
S$_3$···H$_8$	3.373(28)	3.380		0.437	3.266	3.221
S$_3$···H$_{10}$	4.180(19)	4.183		0.142	4.170	4.185
S$_3$···H$_{11}$	4.647(14)	4.651		0.212	4.536	4.597
S$_3$···H$_{12}$	4.647(16)	4.651		0.144	4.716	4.696

[a] Distances (r) and rms vibrational amplitudes (l) are in Å. [b−d] These vibrational amplitudes were refined together in the assigned groups as shown. [e] Calculated from the MP2/6-31+G(d,p) force field (C_1). [f] MP2/6-31+G(d,p). [g] MP4(SDQ)/6-31+G(2d,p).

TABLE 5: Selected Bonding and Nonbonding Interatomic Distances and Vibrational Amplitudes from GED Refinements, along with Corresponding MP2 and MP4(SDQ) Distances for *N*,*N*-Dimethylthiocarbamoyl Chloride (TCC; Symmetry C_1)[a]

	GED				theoretical calculations	
	r_α	r_g	l_{exp}	l_{calc}[g]	r_e[h]	r_e[i]
Bonding						
r(C═S)	1.637(3)	1.641	0.049(5)	0.044	1.638	1.649
r(C_2−N)	1.343(4)	1.348	0.047(4)[b]	0.045	1.355	1.341
r(C_5−N)	1.456(3)	1.468	0.051(4)[b]	0.049	1.463	1.467
r(C_9−N)	1.459(3)	1.476	0.051(4)[b]	0.050	1.465	1.469
r(C_2−Cl)	1.768(4)	1.772	0.062(6)	0.054	1.769	1.783
Torsion Independent						
$N_1 \cdot S_3$	2.675(9)	2.680		0.056	2.673	2.678
$N_1 \cdot Cl_4$	2.604(7)	2.608	0.068(10)[c]	0.063	2.615	2.618
$C_2 \cdot C_5$	2.409(8)	2.416	0.059(11)[d]	0.064	2.403	2.400
$C_2 \cdot C_9$	2.489(7)	2.496	0.060(11)[d]	0.065	2.485	2.476
$C_5 \cdot C_9$	2.472(19)	2.489	0.082(11)[d]	0.087	2.509	2.531
$S_3 \cdot Cl_4$	2.944(5)	2.948	0.075(4)[e]	0.064	2.959	2.973
Torsion Dependent						
Two Angles						
$C_5 \cdot\cdot S_3$	3.041(21)	3.048	0.111(7)[f]	0.101	2.992	3.006
$C_9 \cdot\cdot S_3$	4.038(8)	4.040	0.077(7)[f]	0.067	4.029	4.043
$C_5 \cdot\cdot Cl_4$	3.986(9)	3.988	0.078(7)[f]	0.067	3.992	4.005
$C_9 \cdot\cdot Cl_4$	2.911(22)	2.920	0.131(8)[f]	0.121	2.897	2.883
$C_2 \cdot\cdot H_6$	3.305(15)	3.314		0.101	3.292	3.293
$C_2 \cdot\cdot H_7$	2.750(24)	2.765		0.245	2.753	2.700
$C_2 \cdot\cdot H_8$	2.658(25)	2.673		0.207	2.643	2.700
$C_2 \cdot\cdot H_{10}$	3.354(16)	3.363		0.102	3.337	3.334
$C_2 \cdot\cdot H_{11}$	2.864(23)	2.881		0.201	2.763	2.817
$C_2 \cdot\cdot H_{12}$	2.760(26)	2.778		0.260	2.880	2.816
Three Angles						
$Cl_4 \cdots H_6$	4.686(21)	4.690		0.118	4.688	4.699
$Cl_4 \cdots H_7$	4.331(79)	4.337		0.209	4.357	4.364
$Cl_4 \cdots H_8$	4.346(26)	4.352		0.186	4.332	4.364
$Cl_4 \cdots H_{10}$	3.992(28)	4.001		0.113	3.952	3.963
$Cl_4 \cdots H_{11}$	2.895(81)	2.919		0.338	2.617	2.803
$Cl_4 \cdots H_{12}$	2.748(111)	2.767		0.581	3.040	2.803
$S_3 \cdots H_6$	4.112(19)	4.120		0.113	4.060	4.084
$S_3 \cdots H_7$	3.091(88)	3.106		0.438	3.028	2.913
$S_3 \cdots H_8$	2.825(61)	2.843		0.313	2.769	2.913
$S_3 \cdots H_{10}$	4.759(24)	4.763		0.112	4.746	4.758
$S_3 \cdots H_{11}$	4.439(47)	4.446		0.183	4.379	4.397
$S_3 \cdots H_{12}$	4.318(59)	4.325		0.240	4.373	4.397

[a] Distances (r) and rms vibrational amplitudes (l) are in Å. [b−f] These vibrational amplitudes were refined together in the assigned groups as shown. [g] Calculated from the MP2/6-31+G(d,p) force field (C_1). [h] MP2/6-31+G(d,p). [i] MP4(SDQ)/6-31+G(2d,p).

(anti), respectively. However, in the chloro-substituted molecule TCC, we found that the calculated N−Me barrier anti to C═S (i.e., syn to C−Cl) bond was much lower in energy, at only 0.07 kcal mol^{-1}, compared to 0.53 kcal mol^{-1} for the bond syn to C═S (i.e., anti to C−Cl), see Table 2. In addition to the obvious differences due to the halogenation in TCC, it should also be recalled that the minimum-energy orientation of the *N*,*N*-dimethyl groups were found to be different in the two thioamide molecules, see Figure 1.

Even though the MP4(SDQ) and the DFT/B3LYP calculations gave essentially planar molecular structures for TFA and TCC, optimizations based on the inclusion of a true mirror plane showed that the equilibrium structures did not exhibit C_s symmetry properties. In Figure 6 is shown a series of four rotamers valid for both molecules, displaying the label system used in this work. Assuming the MP2-based frequency calculations to give the more correct properties of the obtained C_s stationary points, it was found that the HF calculations gave false rotamer minima in several cases. For instance, the C_s-constrained rotamer (180, 0) in Figure 6 had no imaginary frequencies for TFA and TCC using the HF method, while the MP2 method showed that this rotamer structure was not a true minimum for either of the molecules. The HF calculations also gave no imaginary frequencies for C_s-constrained rotamer (180, 180) in Figure 6 for TCC, while again the MP2 calculations gave one imaginary frequency. All of the MP2 calculations under a C_s symmetry constraint gave imaginary frequencies, thereby indicating that none of the rotamer equilibrium structures exhibited true C_s symmetry in the ground state.

In Table 8, the experimental GED results for TFA and TCC from the present work are shown together with the results for *N*,*N*-dimethylformamide,[6] *N*,*N*-dimethylcarbamoyl chloride[7] and the previous results for TCC as reported by Naumov et al.[8] We have previously discussed the contraction of the r(C(X)−N) bond distance (X = O, S) on going from the amides to the corresponding thioamides, which was in accordance with the assumed relative contributions of the resonance forms **B** and **D** shown in Scheme 1, and the resulting higher rotational energy barrier in the thioamides. However, on comparison of only the results for TFA and TCC in the present work, there was no corresponding contraction in this bond distance due to the substitution of the H atom for the Cl atom; the values were r_g(C(S)−N) = 1.346(2) Å in TFA and r_g(C(S)−N) = 1.348(4) Å in TCC, whereas in the amides (X = O) the corresponding values were (r_g) 1.391(7) Å in the formamide[6] contracted to 1.365(3) Å in the chlorinated compound,[7] see Table 8. The observed noncontracting behavior of r(C(S)−N) in the thioamides when comparing only TFA and TCC was in agreement with both the MP2 and MP4(SDQ) results, see Tables 4 and 5. However, the observed contraction in the r(C(X)−N) bond when comparing the amides (X = O)[6,7] with the corresponding TFA and TCC thioamides (X = S) were reproduced at the MP2/6-31+G(d,p) level of theory. Also, it was seen from Table 8 that there were some significant differences between the previously reported results for TCC[8] and the results in the present work. The r_g(C═S) bond distance was found to be significantly higher in the previous work,[8] having a r_g value of 1.652(5) Å compared to 1.641(3) Å observed for TCC in the present work. The value from the MP4(SDQ) calculations was 1.649 Å, whereas it was 1.638 Å at the MP2 level, see Table 5. However, when we study the calculated r(C═S) bond distance values for TFA, see Table 4, the calculations (MP2, MP4(SDQ)) indicated a slight contraction in this parameter value when going from TFA to the TCC molecule. This contraction was reproduced by the present GED analyses, showing the observed value of r_g(C═S) = 1.649(2) Å in TFA compared to the lower value of r_g(C═S) = 1.641(3) Å in TCC, see Table 8. In the work on TCC by Naumov et al.,[8] they also reported an observed value for r_g(C(S)−N) = 1.334(3) Å, which was significantly lower than the result in the present work (r_g(C(S)−N) = 1.348(4) Å). The ab initio MO and DFT calculations ranged in this case from 1.341 Å (MP4(SDQ)) and 1.347 Å (DFT/B3LYP) to the value of 1.355 Å from the MP2 results for TCC. Thus our GED observations seemed more in agreement with the range of calculated ab initio MO and DFT values for the central r(C(S)−N) bond distance, see Tables 3 and 5. Also, Naumov et al. calculated the charges on the heavy atoms for TCC and its amide counterpart, *N*,*N*-dimethylcarbamoyl chloride,[8] and the differences seen for the charges between the two molecules were much in accordance with the resonance arguments set forward previously in the present article. For instance, it may be seen from Table 5 in the work by Naumov et al. that the charge on the nitrogen atom increases from −0.65 D to a near zero value of −0.09 D from MP2 calculations[8] when comparing the amide and the thioamide (TCC; slightly different basis sets used). The

TABLE 6: Correlation Matrix (×100) for the Refined Parameters of *N,N*-Dimethylthioformamide (TFA)

parameter	σ_{LS}[a]	r_1	r_2	r_3	r_4	$\angle_1$	$\angle_2$	$\angle_3$	ϕ_1	l_1	l_2	l_3	l_4	l_5	l_6
r(C═S)	0.06	100													
r(C_2−N)	0.07	16	100												
r(⟨$C_{5,9}$−N⟩)	0.04	26	45	100											
r(⟨C−H⟩)	0.13	−15	20	9	100										
∠NC_2S	9.4	−38	−41	−9	8	100									
∠⟨$C_2NC_{5,9}$⟩	16.3	−11	−20	−34	−10	−46	100								
∠⟨$NC_{5,9}H$⟩	24.4	−18	−10	−15	−22	−17	27	100							
ϕ_1(C_2−N)	93.9	−23	−26	−26	1	26	−1	−5	100						
l_1(C═S)	0.05	−12	−30	−34	3	15	7	9	17	100					
l_2(C_2−N)	0.06	51	2	5	−19	−11	−9	−10	−6	6	100				
l_3(C_2−H_4)	0.10	4	16	22	1	1	−11	−4	−6	−4	10	100			
l_4(N·S)	0.08	−4	−25	−16	−3	13	5	12	3	22	8	4	100		
l_5(C_2·C_5)	0.09	7	−8	−10	4	6	12	−27	13	14	16	0	10	100	
l_6(C_5··S)	0.12	5	−8	1	3	7	−11	−9	4	16	13	4	4	13	100

[a] Standard deviations (×100) from least-squares refinement. Distances (r) and amplitudes (l) are in Å; angles (∠, ϕ) are in deg.

TABLE 7: Correlation Matrix (×100) for the Refined Parameters of *N,N*-Dimethylthiocarbamoyl Chloride (TCC)

parameter	σ_{LS}[a]	r_1	r_2	r_3	r_4	r_5	$\angle_1$	$\angle_2$	$\angle_3$	$\angle_4$	ϕ_1	l_1	l_2	l_3	l_4	l_5	l_6	l_7	l_8
r(C═S)	0.11	100																	
r(C_2−N)	0.15	−7	100																
r(⟨$C_{5,9}$−N⟩)	0.10	23	44	100															
r(⟨C−H⟩)	0.28	−21	22	7	100														
r(C_2−Cl_4)	0.13	34	−33	0	−13	100													
∠NC_2S	21.1	35	−22	−8	−6	69	100												
∠⟨$C_2NC_{5,9}$⟩	21.6	−35	−31	−45	4	−18	1	100											
∠NC_2Cl	15.9	8	14	24	−2	−35	−74	−5	100										
∠⟨$NC_{5,9}H$⟩	53.4	−5	−13	−27	−22	17	14	9	−16	100									
ϕ_1(C_2−N)	355.4	22	32	42	12	7	10	−10	25	−13	100								
l_1(C═S)	0.14	6	−31	−52	−3	6	20	26	−20	22	−18	100							
l_2(C_2−N)	0.14	49	−25	−16	−20	27	34	−2	−12	3	1	49	100						
l_3(C_2−Cl_4)	0.18	14	−27	−41	−3	10	21	19	−17	25	−11	80	47	100					
l_4(C_5−H)	0.23	−8	18	16	6	−8	−1	−1	0	−9	10	−5	−6	−1	100				
l_5(N·Cl)	0.35	−53	−22	−14	8	−48	−63	32	34	−17	−17	5	−19	−1	4	100			
l_6(C_5··C_2)	0.36	−41	−28	−27	8	−33	−18	55	−6	−22	−15	20	−2	14	3	7	100		
l_7(C_5··S)	0.20	−20	−24	−19	4	−3	−22	12	10	0	−18	21	6	17	1	37	23	100	
l_8(S·Cl)	0.11	−18	−28	−23	6	−9	−14	4	3	−4	−30	26	12	22	6	31	19	29	100

[a] Standard deviations (×100) from least-squares refinement. Distances (r) and amplitudes (l) are in Å; angles (∠, ϕ) are in deg.

TABLE 8: Comparison of Experimental Structural Results from Gas Electron Diffraction (GED) for Selected *N,N*-Dimethylformamides and *N,N*-Dimethylthioformamides[a]

	H−C(O)−$N(CH_3)_2$	H−C(S)−$N(CH_3)_2$ (TFA)	Cl−C(O)−$N(CH_3)_2$	Cl−C(S)−$N(CH_3)_2$ (TCC)	Cl−C(S)−$N(CH_3)_2$ (TCC)
r_g(C═X)[b]	1.224(3)	1.649(2)	1.202(3)	1.641(3)	1.652(5)
r_g(C(X)−N)[b]	1.391(7)	1.346(2)	1.365(3)	1.348(4)	1.334(3)
r_g(⟨C_{Me}−N⟩)	1.453(4)	1.463(2)	1.462(5)	1.472(3)	1.475(3)
r_g(C−Cl)			1.789(4)	1.772(4)	1.769(5)
∠NCX[b]	123.5(6)	127.0(3)	126.5(2)	127.4(6)	125.8(6)
∠$CNC_{(syn)}$[c]	120.8(3)	121.6(5)	116.0(4)	118.7(6)	119.3(3)
∠$CNC_{(anti)}$[c]	122.3(4)	122.2(5)	124.8(4)	125.3(6)	124.2(13)
∠NCCl			113.9(3)	113.0(4)	115.2(13)
∠$C_{Me}NC_{Me}$	113.9(5)	116.2(9)	116.2(3)	116.0(12)	116.2[f]
∠XCCl[b]			119.6(2)	119.6(4)	118.9[f]
∠⟨$NC_{Me}H$⟩	110.1(3)	110.4(7)	110.8(3)	109.6(15)	107.5(9)
ϕ_1(C−N)[d]	−16.3(45)	12.8(27)	13.0(25)	−5.5(101)	[0.0]
ϕ_2(N−C_{Me})[d]	25.4(37)	[−163.5][g]	−11.7(40)	[173.2][g]	[180.0]
ϕ_3(N−C_{Me})[d]	−13.1(37)	[12.7][g]	45.3(24)[e]	[−171.4][g]	[180.0]
rotamer type	(0, 0)	(180, 0)	(0, 180)	(180, 180)	(180, 180)
reference	6	present work	7	present work	8

[a] Bond distances are in Å; valence and torsional angles are in deg. [b] X = O, S. [c] Syn and anti refer to the position of C_{Me} relative to the C═X bond (X = O, S). [d] Torsion angles for rotation about the central C−N bond and the two N−C_{Me} bonds. See the text for details. [e] This is the reported value,[7] which conforms to a value of 165.3(24)° according to the definitions used in the present article (cf. rotamer type). [f] Dependent values reported with no standard errors given.[8] [g] Fixed values from the MP2/6-31+G(d,p) calculations in the present work.

diminishing negative charge on the N atom when going from the amide to the thioamide was in accordance with the increasing relative contribution of resonance form **D** in Scheme 1 for the thioamide. When a similar comparison was made for the charges on the C(X) atom (X = O, S), a similar conclusion was reached, supporting the stated resonance picture of these molecules.

In conclusion, we would like to point out the major minimum-energy rotamer pattern for the methyl torsions in the two amides studied by I. Hargittai and G. Schultz[6,7] and the two thioamides TFA and TCC in our work. The following *N,N*-dimethyl minimum-energy rotamers were found from these studies (in (ϕ_2, ϕ_3) label-type form, see Figure 6): (a) H−C(═O)−

$N(CH_3)_2$) (0, 0); (b) Cl−C(=O)−$N(CH_3)_2$) (0, 180); (c) H−C(=S)−$N(CH_3)_2$) (180, 0); (d) Cl−C(=S)−$N(CH_3)_2$) (180, 180). In other words, the presence of the oxygen atom created a zero orientation for the *syn*-methyl group, while a sulfur atom created a 180 orientation for this methyl group. A hydrogen atom in the R′ position, on the other hand, created a zero orientation for the *anti*-methyl group (anti to the C=X; X = O, S), while substitution for the chlorine atom gave the 180 orientation for this methyl group. However, it should be noted that for the thioamides, these conclusions rest solely on the MP2- and MP4(SDQ) ab initio MO calculations. We believe steric factors were of some importance, in addition to the slight hydrogen bonding discussed by I. Hargittai and G. Schultz,[6,7] which will not be present in the thioamides. Together these factors should explain most of the observed behavior in the methyl group orientations of these amide and thioamide classes of molecules.

Acknowledgment. We are very grateful to Professor Kenneth W. Hedberg for use of the Oregon State University GED apparatus. We are also grateful to Dr. Alan D. Richardson for significant help with the recording of the experimental GED data. This work has received support from National Science Foundation under Grant CHE99-87359 and from The Research Council of Norway (Program for Supercomputing) through grants of computing time.

References and Notes

(1) Sugisaki, R.; Tanaka, T.; Hirota, E. *J. Mol. Spectrosc*. **1974**, *49*, 241.
(2) Hargittai, M.; Samdal, S.; Seip, R. *J. Mol. Struct*. **1981**, *71*, 147.
(3) Jackman, L. M. Rotation about partial double bonds in organic molecules. In *Dynamic Nuclear Magnetic Resonance Spectroscopy*; Jackman, L. M., Cotton, F. A., Eds.; Academic: New York, 1975; p 203.
(4) Feigel, M. *J. Phys. Chem*. **1983**, *87*, 3054.
(5) Kitano, M.; Kuchitsu, K. *Bull. Chem. Soc. Jpn*. **1973**, *46*, 3048.
(6) Schultz, G.; Hargittai, I. *J. Phys. Chem*. **1993**, *97*, 4966.
(7) Schultz, G.; Hargittai, I. *J. Phys. Chem*. **1995**, *99*, 11412.
(8) Naumov, V. A.; Ziatdinova, R. N.; Tafipolskii, M. A.; Novikov, V. P. *J. Struct. Chem. (Engl. Transl.)* **2000**, *41*, 531.
(9) Hagen, K.; Hedberg, K. *J. Am. Chem. Soc*. **1973**, *95*, 1003.
(10) Andersen, B.; Seip, H. M.; Strand, T. G.; Stølevik, R. *Acta Chem. Scand*. **1969**, *23*, 3224.
(11) Gundersen, G.; Hedberg, K. *J. Chem. Phys*. **1969**, *51*, 2500.
(12) Hedberg, L. *Abstracts of Papers*, 5th Austin Symposium on Gas-Phase Molecular Structure, Austin, TX, March 1974; p 37.
(13) Ross, A. W.; Fink, M.; Hilderbrandt, R. *International Tables of Crystallography*; Kluwer Academic Publishers: Dordrecht, Netherlands, 1992; Vol. 4, p 245.
(14) Frisch, M. J.; Trucks, G. W.; Schlegel, H. B.; Scuseria, G. E.; Robb, M. A.; Cheeseman, J. R.; Zakrzewski, V. G.; Montgomery, J. A., Jr.; Stratmann, R. E.; Burant, J. C.; Dapprich, S.; Millam, J. M.; Daniels, A. D.; Kudin, K. N.; Strain, M. C.; Farkas, O.; Tomasi, J.; Barone, V.; Cossi, M.; Cammi, R.; Mennucci, B.; Pomelli, C.; Adamo, C.; Clifford, S.; Ochterski, J.; Petersson, G. A.; Ayala, P. Y.; Cui, Q.; Morokuma, K.; Malick, D. K.; Rabuck, A. D.; Raghavachari, K.; Foresman, J. B.; Cioslowski, J.; Ortiz, J. V.; Stefanov, B. B.; Liu, G.; Liashenko, A.; Piskorz, P.; Komaromi, I.; Gomperts, R.; Martin, R. L.; Fox, D. J.; Keith, T.; Al-Laham, M. A.; Peng, C. Y.; Nanayakkara, A.; Gonzalez, C.; Challacombe, M.; Gill, P. M. W.; Johnson, B. G.; Chen, W.; Wong, M. W.; Andres, J. L.; Head-Gordon, M.; Replogle, E. S.; Pople, J. A. *Gaussian 98*, revision A.9; Gaussian, Inc.: Pittsburgh, PA, 1998.
(15) Van Hemelrijk, D.; Van den Enden, L.; Geise, H. J.; Sellers, H. L.; Schäfer, L. *J. Am. Chem. Soc.* **1980**, *102*, 2189.
(16) Schäfer, L.; Ewbank, J. D.; Siam, K.; Chiu, N.; Sellers, H. L. In *Stereochemical Applications of Gas-Phase Electron Diffraction*; Hargittai, I., Hargittai, M., Eds.; VCH Publishers: New York, 1988; Part A, p 301.
(17) Klimkowski, V. J.; Ewbank, J. D.; Van Alsenoy, C.; Scardale, J. N.; Schäfer, L. *J. Am. Chem. Soc.* **1982**, *104*, 1476.
(18) Hedberg, L.; Mills, I. M. *J. Mol. Spectrosc*. **1993**, *160*, 117.
(19) Hedberg, L.; Mills, I. M. *J. Mol. Spectrosc*. **2000**, *203*, 82.
(20) Hedberg, K.; Iwasaki, M. *Acta Crystallogr*. **1964**, *17*, 529.
(21) Bartell, L. S. *J. Chem. Phys*. **1963**, *38*, 1827.
(22) Kuchitsu, K.; Morino, Y. *Bull. Chem. Soc. Jpn*. **1965**, *38*, 841.
(23) Wiberg, K. B.; Rablen, P. R.; Rush, D. J.; Keith, T. A. *J. Am. Chem. Soc*. **1995**, *117*, 4261.